Izvestiya, Atmospheric and Oceanic Physics, Vol. 40, No. 6, 2004, pp. 737–746. Translated from Izvestiya AN. Fizika Atmosfery i Okeana, Vol. 40, No. 6, 2004, pp. 821–831.

Synchronous Variations in the Caspian Sea Level from Coastal Observations in 1977–1991

A. A. Lyubushin*, V. F. Pisarenko, M. V. Bolgov***, M. V. Rodkin****, and T. A. Rukavishnikova****

** Schmidt United Institute of Physics of the Earth, Russian Academy of Sciences, Bol'shaya Gruzinskaya ul. 10, Moscow, 123995 Russia*
e-mail: lubushin@mtu-net.ru
*** International Institute of Earthquake Prediction Theory and Mathematical Geophysics, Russian Academy of Sciences, Varshavskoe sh. 79/2, Moscow, 113556 Russia*
e-mail: pisarenko@yaol.ru; tanyar@sirius.mitp.ru
**** Institute of Water Problems, Russian Academy of Sciences, ul. Gubkina 3, Moscow, 119991 Russia*
e-mail: caspian-sea@mtu-net.ru
***** Geophysical Center, Schmidt United Institute of Physics of the Earth, Russian Academy of Sciences, ul. Molodezhnaya 3, Moscow, 117296 Russia*
e-mail: rodkin@wdcb.ru
Received July 10, 2003; in final form, September 30, 2003

Abstract—The time series of variations in the Caspian Sea level derived from synchronous measurements at 15 coastal stations with a sampling interval of 6 h over the period of observations from the beginning of 1977 to the end of 1991 are considered. Collective (common) components of both stationary and nonstationary character were to be recognized in this 15-dimensional time series. Nonstandard multidimensional spectral methods of the estimation of canonical coherences in a moving time window, as well as the spectral analysis of aggregated signals, were used to analyze the data. This analysis detected common harmonic components forming semidiurnal and diurnal groups of tidal harmonics, seasonal variations, and the frequency band of variations with a strong coherence in the range of periods from 4 to 8 days. Additionally, we identified a common low-frequency harmonic with a period of 12.85 yr, which is supposedly associated with the influence of cyclic changes of a global character on variations in the Caspian Sea level.

INTRODUCTION

The Caspian Sea, being an enclosed water body unique in its dimensions, has a hydrologic regime characterized by specific features, such as an increased (compared to the World Ocean) amplitude of variations in the water level, which was equal to about 4 m over the past century (the period of instrumental observations).

Visual analysis of the Caspian Sea level trend on time scales exceeding one year can lead to the conclusion that the variations resemble a trajectory of Brownian motion; however, the physical mechanisms responsible for level variations are much more complicated. Stochastic oscillations of the climate, both natural and anthropogenic, are the main cause of the large amplitude of variations and, as a consequence, the uncertainty of long-term hydrologic predictions.

Variations in the level of an inland water body without outflow are a weakly predictable natural phenomenon, which, nevertheless, can be described in terms of stochastic models of hydrometeorological processes and ideas of the water budget of such a body. In studies of sea-level variations, the dynamic variations caused by inducing processes of a synoptic scale (wind, atmospheric pressure) are traditionally considered separately from eustatic changes resulting from the accumulation or discharge of water in a sea over various time intervals.

The mechanism of eustatic variations in the level of a completely impounded water body consists in the following. The water supplied into a water body in the form of river inflow and precipitation is mainly spent on evaporation. When the total water inflow exceeds evaporation, the water body level rises, which leads to an increase in the water table and, consequently, in the growth of evaporation. If evaporation exceeds the inflow, the level drops, and the evaporating surface decreases. Accordingly, evaporation also decreases, slowing down the rate of water level lowering. This is the reason why, under stationary climatic conditions, the level of an inland water body oscillates near the position corresponding to the equality of the average long-term values (volumes) of the inflow and evaporation (the so-called gravity level).

Rises and drops in the water level due to wind, seiches, and tidal oscillations are usually regarded as

dynamic variations in the Caspian Sea level. The analysis of seiche variations performed in [1] and based on spectral analysis of observation series of various lengths made it possible to identify the periods of single-node (8.66 h) and double-node (4.39 h) seiches. In the middle and southern parts of the Caspian Sea, seiches with periods of 2 and 6 days are recognizable. The analysis of tidal oscillations performed by several authors and based on the processing of mareographic records showed that a semidiurnal tide with a period close to 12.4 h, insignificant in its magnitude, dominates in the Caspian Sea. Nonperiodic off-and-on water oscillations are mainly controlled by wind characteristics and the bottom topography in the coastal part of the sea.

The various sea-level variations listed above are, as a rule, separately accounted for in applied problems, which dictates the use of different models in different frequency ranges. Nevertheless, the problem of constructing a general stochastic model of variations in the Caspian Sea level remains open, which induced the authors of this paper to make an attempt at performing multidimensional spectral analysis of the data of sea-level observations over the period of sea-level rise with the use of the advanced methods of estimation.

METHODS OF DETECTING COLLECTIVE SIGNALS

Below, we briefly outline two methods of revealing collective variations in the behavior of scalar components of the multidimensional time series used in this paper. The first method is intended for determination of the time intervals and frequency bands in which a nonstationary synchronizing signal is observed. This method was initially developed for solving the problems of the search for precursors of strong earthquakes from the data provided by the systems of geophysical monitoring [2, 3]. The physical meaning of the method consists in searching for the frequency bands and time intervals where the collective behavior of jointly analyzed processes is enhanced. Interest in the enhancement of collectivism in variations of either different processes or the same process measured at different points (the present case) is related to the methodical recommendations stemming from the most common regular features in the behavior of the systems approaching bifurcation. An increase in the correlation radius of fluctuations in the vicinity of the bifurcation point indicates that the system tends to establish the coordination in its entire volume, thereby preparing itself for the collective transition to a new state [4]. Of course, no search for precursors of any catastrophes was implied when the data on variations in the Caspian Sea level were analyzed; however, the method itself has a wider sphere of applicability. In this case, hidden, possibly nonstationary, variations in the level of the sea that encompass its entire water area were of interest to us.

The second method (of aggregated signals) is intended for the recognition of common stationary harmonic oscillations and is based on the analysis not in a moving time window of a relatively short length but in the whole available sample. This method was developed for solving the problems of the search for the signals controlling the duration of long-term phases of earthquake preparation [5] and used the Fourier expansion of the initial time series. The well-aggregated signal can be defined as such a scalar signal, which accumulates to the maximum extent the most common variations simultaneously existing in all analyzed processes and, at the same time, suppresses the components characteristic of only one process. The aggregated signal is constructed in two stages. At the first stage, the initial multidimensional series is replaced by the multidimensional series, the so-called canonical components, which retain common signals and are free of local signals. At the second stage, the common signals are additionally enhanced by the construction of a single scalar series (their first principal component), which is called the aggregated signal of the initial multidimensional time series. Either stage of the aggregation is realized as the succession of the projections of multidimensional Fourier transforms on the eigenvectors of various spectral matrices. Note that the modification of the method of aggregated signals with the use of wavelet transforms instead of the Fourier transform allows the recognition of nonstationary short-lived common signals (synchronous bursts) [6]; however, this modification cannot be applied to the data under consideration.

It should be noted that the first method of estimation in a moving time window was used in [7] to analyze the collective effects in variations in the runoff of the rivers of Europe and the European part of the former USSR and a possible relation of these effects to global climatic variations.

An ordinary spectrum of the coherence of two processes can be nonrigorously defined as the square of the correlation coefficient for these processes at the frequency ω [8]. The canonical coherences represent a generalization of the concept of the coherence spectrum to the situation when, instead of a pair of scalar time series, it is necessary to investigate the relation between two vector time series: the m-dimensional series $X(t)$ and the n-dimensional series $Y(t)$, at different frequencies. The quantity $\mu_1^2(\omega)$ called the square of the modulus of the first (maximum) canonical coherence of the series $X(t)$ and $Y(t)$, which replaces an ordinary coherence spectrum in this case, is calculated as the maximum eigenvalue of the matrix

$$U(\omega) = S_{xx}^{-1}(\omega)S_{xy}(\omega)S_{yy}^{-1}(\omega)S_{yx}(\omega) \qquad (1)$$

[9, 10]. Here, t is the discrete time numbering the successive counts, ω is the frequency, $S_{xx}(\omega)$ is the spectral matrix with the size $m \times m$ of the time series $X(t)$, $S_{xy}(\omega)$ is the cross-spectral rectangular matrix with the size

$m \times n$, $S_{yx}(\omega) = S_{xy}^H(\omega)$, and H is the sign of the Hermitian conjugation. From the applied standpoint, the quantity $\mu_1^2(\omega)$ replaces the square of the modulus of the coherence spectrum in the case of two multidimensional signals.

We now introduce the concept of the component-by-component canonical coherences $\nu_i^2(\omega)$ of the q-dimensional time series $Z(t)$ as the squares of the moduli of the maximum canonical coherence in the situation when, in formula (1), the ith scalar component of the q-dimensional series $Z(t)$ is assumed to be the series $Y(t)$ and the $(q-1)$-dimensional series consisting of the other components is assumed to be the $X(t)$ series. Therefore, the quantity $\nu_i^2(\omega)$ characterizes the coherence of variations in the ith component with variations in the set of all the other components at the frequency ω. The introduction of the component-by-component canonical coherence makes it possible to determine one more frequency-dependent statistics $\kappa(\omega)$, which characterizes the coherence of variations in all the components of the vector series $Z(t)$ at the frequency ω:

$$\kappa(\omega) = \prod_{i=1}^{q} \nu_i(\omega). \tag{2}$$

Note that, by virtue of the construction, the value of $\kappa(\omega)$ belongs to the interval $\{0, 1\}$, and the closer the corresponding value to one, the stronger the relation between variations in the components of the multidimensional time series $Z(t)$ at the frequency ω. Frequency-dependent quantity (2) can be called *the spectral measure of the coherence of a multidimensional time series.*

In order to estimate the temporal variability of the interaction of recorded processes, it is necessary to perform calculations in the moving time window of a specified length. Let τ be the time coordinate of the window having a length of L counts. Calculating the spectral matrices for the samples falling in the time window τ, we obtain the two-parameter function $\kappa(\tau, \omega)$. The bursts of the $\kappa(\tau, \omega)$ value will determine the frequency bands and time intervals in which the collective behavior of jointly analyzed processes is enhanced.

To realize this algorithm, it is necessary to have the estimate of the spectral matrix $S_{zz}(\tau, \omega)$ with the size $q \times q$ in each time window. Below, we prefer to use the model of vector autoregression [11]. The method consists in the estimation of model parameters:

$$Z(t) + \sum_{k=1}^{p} A_k Z(t-k) = e(t). \tag{3}$$

Here, A_k are the matrices of autoregression parameters with the size $q \times q$; p is the autoregression order; and $e(t)$ is the q-dimensional time series of the residuals of identification, which is assumed to be the sequence of independent Gaussian vectors with a zero mean and an unknown covariance matrix P. It is important to note that model (11) was constructed after the preliminary operations of eliminating the general linear trend and normalizing each scalar component to the unit variance. These operations were performed independently in each time window of processing and for each scalar component of the multidimensional series. Their meaning consists in eliminating the influence of diversification in scale in the series processed. To estimate the matrices A_k and P, the Durbin–Levinson recurrence procedure [11] is used, for which the sampling estimates of the covariance matrices must be preliminarily calculated.

The spectral matrix is estimated by the formula

$$S_{ZZ}(\omega) = F^{-1}(\omega) P F^{-H}(\omega), \quad \text{where}$$
$$F(\omega) = I + \sum_{k=1}^{p} A_k \exp(-i\omega k). \tag{4}$$

Estimate (4) has a rather high resolution in frequency for short samples and, therefore, is more preferable for estimations in a moving time window than, for example, nonparametric estimates in terms of the averaging of multidimensional periodograms. There are no formalized procedures for the choice of the autoregression order p. In the calculations, p was chosen by the trial method as the minimum value, whose further increase does not lead to a substantial change in the main elements of the behavior of the $\kappa(\tau, \omega)$ dependence. Below, we use the value $p = 5$ everywhere.

Further, we describe the formalized construction of the aggregated signal. For this purpose, we will extract the ith scalar component $Z_i(t)$ from the multidimensional series of observations $Z(t)$ and try to filter the $(q-1)$-dimensional series consisting of the residual components in such a way that the scalar signal $C_i^{(Z)}(t)$ obtained at the filter output have the maximum coherence with the extracted series $Z_i(t)$ at each frequency. In order to do this, the components of the eigenvector of matrix (1), where $Z_i(t)$ appears as $Y(t)$ and $Z^{(i)}(t)$ appears as $X(t)$, corresponding to its maximum eigenvalue (obviously equal to $\nu_i^2(\omega)$), should be used as a multidimensional frequency filter. If the component $Z_i(t)$ contains the noise that is characteristic solely of this series and is absent in the other components of the series $Z(t)$, it is absent in the signal $C_i^{(Z)}(t)$ simply by its construction, and this is the meaning of such an operation. At the same time, the series $C_i^{(Z)}(t)$ retains all the components $Z_i(t)$ common for the remaining components of the series $Z(t)$, i.e., the signal $Z^{(i)}(t)$. The signal

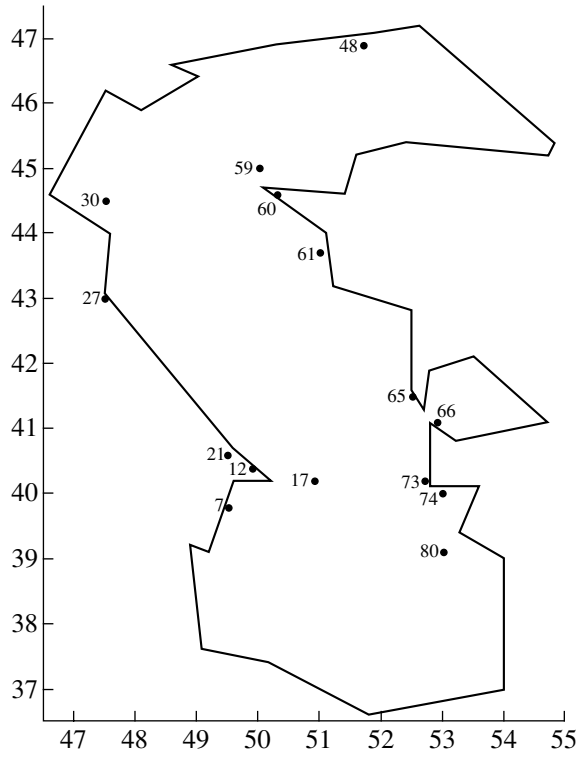

Fig. 1. Numbers and locations of 15 stations on the Caspian Sea coast, whose observations were used in the analysis.

$C_i^{(Z)}(t)$ will be referred to as the canonical component of the scalar series $Z_i(t)$.

We now determine the aggregated signal $A_Z(t)$ of the multidimensional time series $Z(t)$ as the first principal spectral component [9, 10] of the multidimensional series $C^{(Z)}(t)$ composed of the canonical components $C_i^{(Z)}(t)$ of each scalar time series forming the initial series $Z(t)$. Recall that the main spectral component is the projection of the vector of Fourier transforms on the eigenvector of the spectral matrix corresponding to its maximum value. It should be emphasized that the series $A_Z(t)$ differs from the simple first principal component. In either of the cases, the series are determined by multidimensional filterings, in which the eigenvectors of the spectral matrices corresponding to their maximum eigenvalues are assumed to be multidimensional frequency filters. However, for the ordinary first principal component, the matrix of the initial time series $Z(t)$ is such a spectral matrix, whereas the spectral matrix of the series $C^{(Z)}(t)$ is the matrix of the series $A_Z(t)$. Although the common components are extracted in the course of either filtering, the aggregated signal $A_Z(t)$ is preferable, because individual noises are completely eliminated in the course of its construction.

Contrary to the estimation in a moving time window, nonparametric estimation through the frequency averaging of periodograms and cross-periodograms [9, 10] was used to estimate the spectral matrix required for the construction of the aggregated signal. Such a choice was related to a higher structural stability of the classical periodogram estimates of power spectra for long time series [11] compared to parametric autoregression estimates of spectral matrices (4), which are advantageous only for short samples. We used a deep averaging (smoothing) of periodograms in the frequency window with the length equal to 1/32 part of the total number of discrete frequency values. Note that the aggregated signal has no physical dimensionality; since it is constructed after the sequence of operations aimed at the normalization of the initial data, its meaning consists solely in the formal extraction of the most common harmonic variations. The thorough description of all elements of the computational technology can be found in [5].

DATA AND RESULTS OF THEIR ANALYSIS

The arrangement of 15 coastal stations whose observations were used to solve the problem stated is schematically shown in Fig. 1. The numbers of stations are coded; however, for simplification, the standard combination of numerals at the beginning of the codes (970) is omitted. For example, the actual number of station 48 is 97048.

The initial time series represent the sequences of synchronous measurements at a time step of 6 h beginning on January 1, 1977, at 09:00 and continuing to the end of 1991. The total duration of each analyzed series is equal to 21 908 counts. The upper 15 curves in Fig. 2 are the plots of the initial data constructed on the same scale (the scale is shown on the ordinate); the marks on the right relate each curve to the respective observation point. The common seasonal (annual) variations in the Caspian Sea level and the total linear trend reflecting its increase are immediately apparent. Additionally, one should note the presence of intense noise in the data from points 30 and 48, which is due to their location in the northern shallow-water part of the Caspian Sea and, as a consequence, a strong influence of wind-induced water surges on observations.

The second curve from the bottom in Fig. 2 represents the plot of the aggregated signal. In addition to seasonal variations, a low-frequency component with a large amplitude is seen. It was approximated by a harmonic trend with an unknown period, which was determined from the condition of the minimum residual variance. The trend period obtained in such a way was equal to 4691 days, which amounts to approximately 12.85 yr.

Finally, the lowermost curve in Fig. 2 is the plot of the solar activity over the period of observations (daily Wolf numbers). The data are taken from the site: http://sidc.oma.be/html/sunspot.html. The solar activity data are presented for the subsequent discussion of

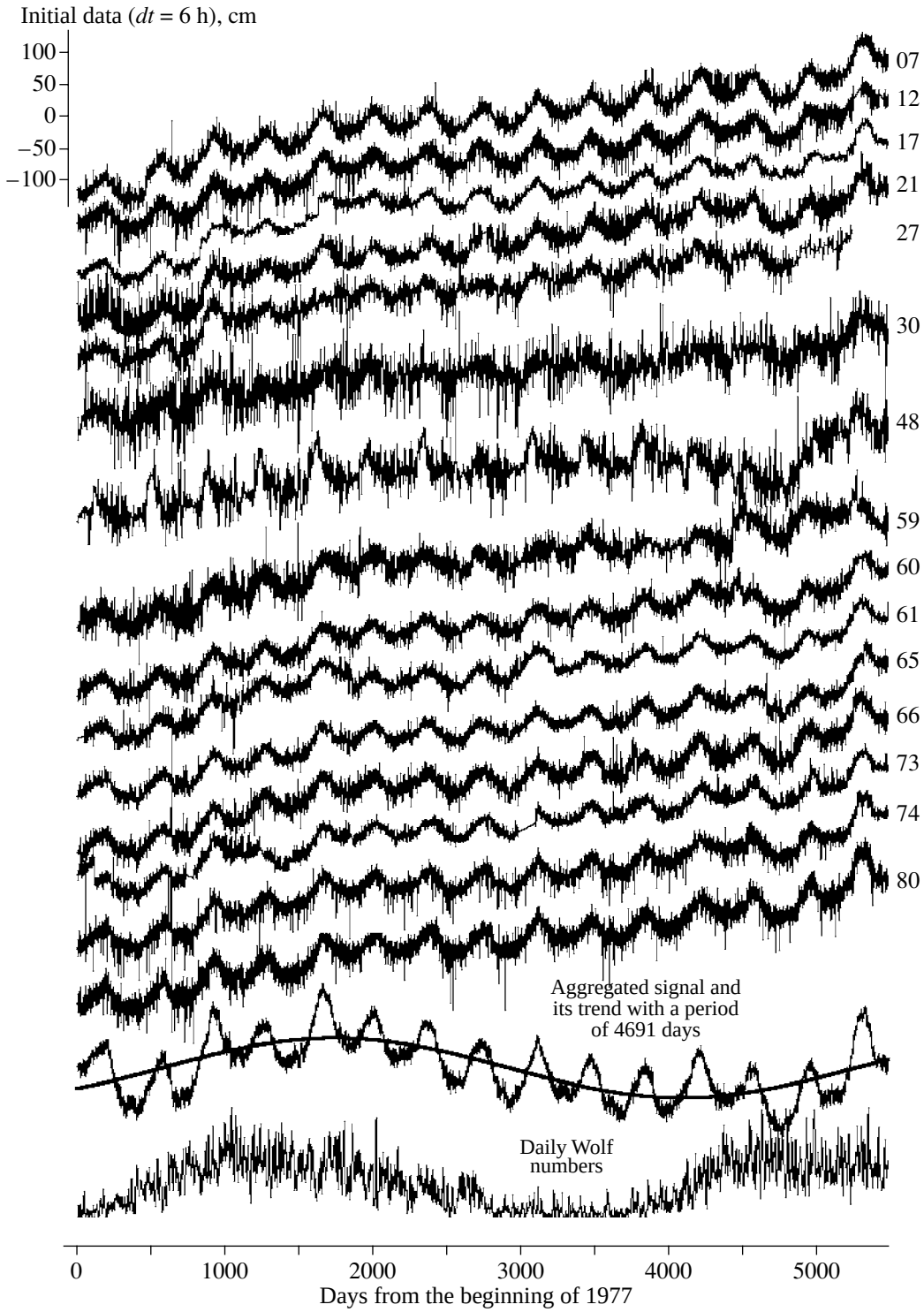

Fig. 2. Plots showing the initial time series (the sampling interval is 6 h; numbers of observation points are indicated nearby), their aggregated signal, and solar activity data (the lowermost plot shows the daily Wolf numbers). The curve showing the harmonic trend with the minimum residual variance, whose period is equal to 4691 days (12.85 yr) is drawn over the plot of the aggregated signal.

a possible origin of the harmonic trend with the period 12.85 yr.

The plots showing the estimates of power spectra of the initial time series after the operations of normalization, i.e., the elimination of the common linear trend and division of each count by the sampling value of the standard deviation, are presented in Fig. 3. Therefore, after the normalization, all signals have the same unit

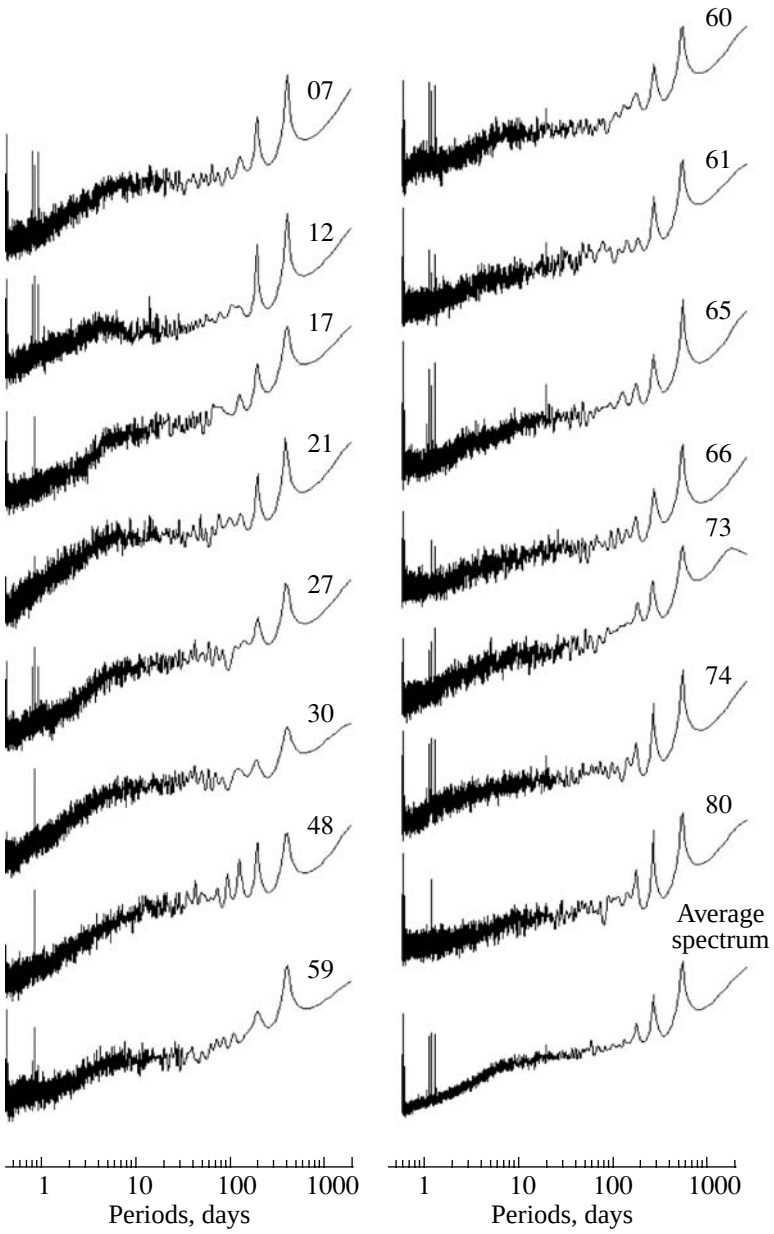

Fig. 3. Plots showing the estimates of the power spectra of the initial time series after applying the operations of normalization (elimination of the common linear trend and division by the sampling standard deviation) and the result of their averaging (the so-called average spectrum).

variance. The normalization does not affect the form of the power spectrum, but instead it becomes possible to calculate the so-called average spectrum (the plot in the lower right-hand corner of Fig. 3) through the arithmetic averaging of the power spectra of all normalized signals for each frequency.

Figure 3 gives the idea of both common and individual features of the behavior of the initial data in the spectral region. Note, in particular, the presence of an indistinctly pronounced "swell," or "corner point," on the plots showing the power spectra in the period range from 4 to 8 days. This feature is most contrasting on the plot showing the power spectrum of observations at point 12. On the plot showing the average spectrum, it is seen as a very diffuse area at the place where the plot changes its slope. Distinctions in the intensities of spectral peaks in the semidiurnal and diurnal groups and in seasonal variations are also intriguing. Note the presence of the spectral peaks corresponding to the annual period and its subharmonics with periods of half-year and one-third of the year appearing due to the fact that the form of annual variations in the sea level differs drastically from a harmonic oscillation.

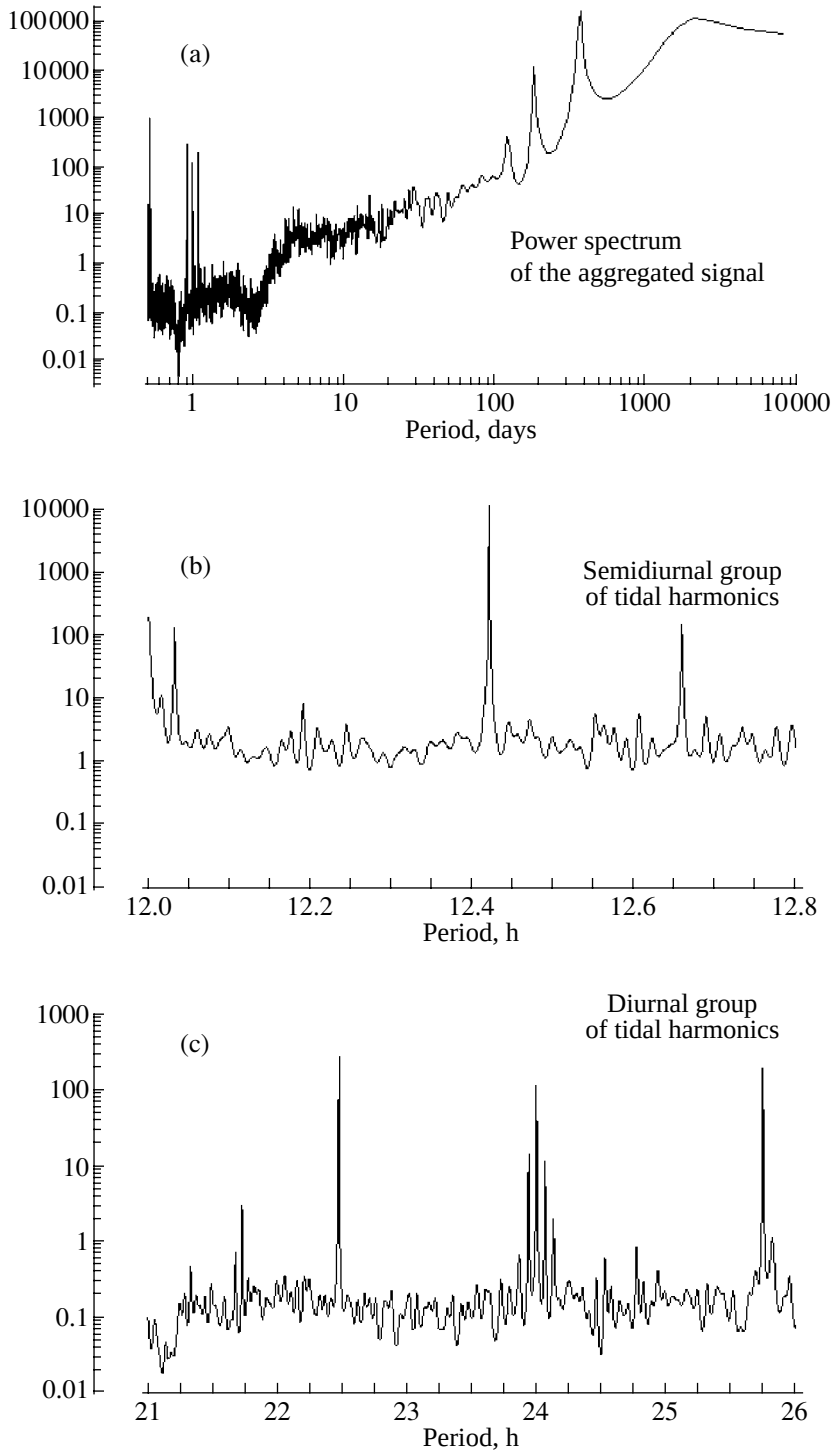

Fig. 4. Plots showing the estimates of the power spectrum of the aggregated signal: (a) for the entire frequency range; (b) for the group of semidiurnal tidal harmonics; and (c) for the group of diurnal tidal harmonics.

The plot showing the estimation of the power spectrum of the aggregated signal for the initial data (the lowermost plot of Fig. 2) is presented in Fig. 4. Recall that the procedure of aggregation emphasizes common spectral components and suppresses individual ones. Due to this procedure, the frequency bands saturated with common spectral components become recognizable in the spectrum of the aggregated signal (Fig. 4a) in the shape of some "hills," whereas the common harmonics produce sharp peaks. The vicinity of the Nyquist frequency (Fig. 4b, the group of semidiurnal tidal variations) and the group of diurnal tidal variations

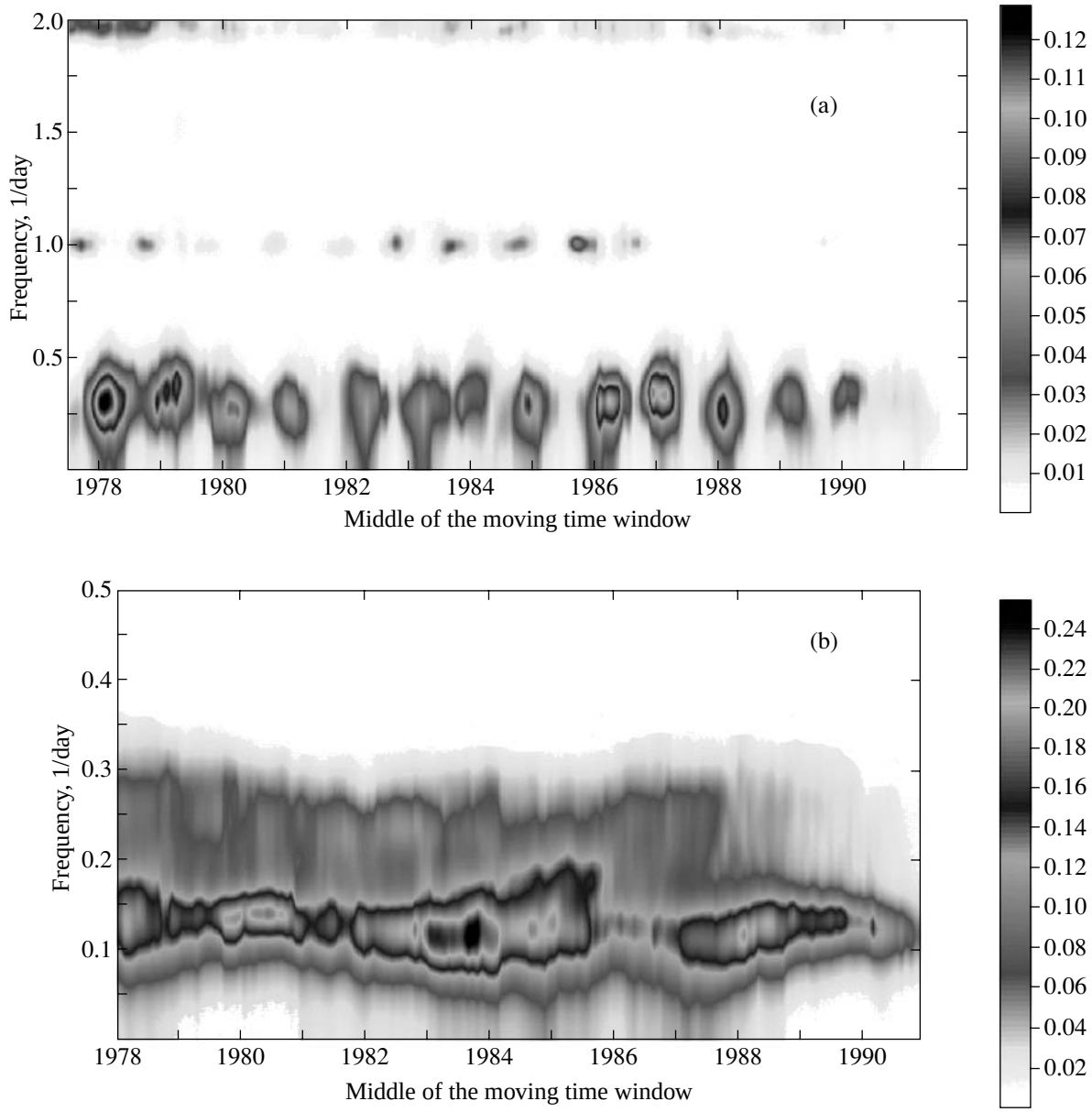

Fig. 5. Product of the component-by-component canonical coherences of the 15-dimensional time series of synchronous measurements of variations in the Caspian Sea level at various coastal stations. The estimation in a moving time window in accordance with the AR vector model of the fifth order: (a) for time series with a sampling interval of 6 h; the time window length is 730 counts (0.5 yr); the time window displacement is 112 counts (28 days, i.e., a lunar month); and (b) for time series after reduction to a sampling interval of 1 day; the time window length is 730 counts (2 yr); the time window displacement is 28 counts (also a lunar month).

(Fig. 4c) are such bands. These groups contain monochromatic components, whose periods are equal to 12.00, 12.03, 12.42, and 12.66 h (a semidiurnal group) and to 21.74, 22.48, 23.94, 24.00, 24.07, 24.13, and 25.74 h (a diurnal group). They are most likely related to lunar–solar tides.

Finally, the period range from 4 to 8 days, which was mentioned when Fig. 3 was discussed, is recognizable in the aggregated signal spectrum as a clearly pronounced flat maximum.

Figure 5 illustrates the results of investigating the nonstationary character of collective effects in level variations. The frequency–time diagram showing the evolution of spectral measure of coherence (2) estimated in the moving time window 730 6-h counts (half-year) is presented in Fig. 5a. The displacement of the neighboring windows was assumed to be 112 counts, which is equal to 28 days. The last value was chosen for reasons of the displacement equality to the lunar month, which makes it possible to place each time window under approximately the same conditions of

changes in the gravity potential. The regular bursts of the measure of coherent behavior falling in mid-winter and summer almost each year in the frequency band with periods ranging from 2 to 4 days can be seen on the diagram presented in Fig. 5a. Note that this band, precisely due to a sharply nonstationary effect of the collective behavior, did not manifest itself in the spectrum of the aggregated signal. As for the vicinities of the diurnal and semidiurnal periods, the bursts of a nonstationary measure of the collective behavior are seen there; however, they are insignificant due to the monochromatic (narrowband) character of common signals of the tidal origin and the closeness of their subharmonics, which are difficult to resolve in frequency because of the relatively small length of the moving time window.

An analogous diagram showing the evolution of spectral measure of coherent behavior (2) estimated for the time series after the elimination of the linear trend and reduction of the sampling interval duration to 1 day (Fig. 3) is presented in Fig. 5b. As before, the time window length was assumed to be equal to 730 counts; however, this time amounts to 2 yr. As for the displacement, it was assumed, as before, to be equal to 28 days, which amounts to 28 counts. A strong coherence and stationary character of the effect of the coherence of variations in the frequency band with periods from 4 to 8 days is, in our opinion, the most noteworthy result. This result is in compliance with the form of the aggregated signal spectrum in Fig. 4a in this range of periods. As for a possible physical mechanism responsible for the appearance of such a strong coherence, the formation of wind seiches simultaneously encompassing the entire Caspian Sea basin should be regarded as the most probable reason.

Note the distinctions between the diagrams shown in Figs. 5a and 5b in the common frequency bands, in particular, the clearly pronounced seasonal variations in Fig. 5a, which are absent in Fig. 5b. To explain this feature, it should be remembered that the time window length in the first case is equal to 0.5 yr; in the second case, to 2 yr. Consequently, with a 2-yr window, the seasonal effect is averaged and produces only a time-uniform increase in the measure of coherence to average values of 0.10–0.12 in the common frequency range.

CONCLUSIONS

The statistical analysis of sea-level variations on the basis of multidimensional spectral methods developed for the recognition of common variations applied to coastal observations of the Caspian Sea level made it possible to identify a number of monochromatic and broadband common components of sea-level variations. The spectral densities obtained partially support the conclusions made previously by different authors on the basis of short-term experimental observations; moreover, new conclusions are also made.

Among the results obtained, stationary strongly coherent variations in the period range from 4 to 8 days, supposedly caused by the wind load on the surface of such a restricted basin as the Caspian Sea, seem to be most striking. The variations in this frequency range are comparable with the duration of the so-called natural synoptic periods [12–14]. Appreciable wind-dependent denivelations appear approximately within two days after the beginning of the wind action and continue from several hours to several days. The following specific feature of the spectra obtained, which takes place virtually at all the stations, is noteworthy: after attaining its maximum value in the period range from 4 to 8 days, the energy does not drop at lower frequencies.

When interpreting the generalized spectra obtained, it should be borne in mind that the river inflow into the Caspian Sea is strongly regulated by water storage reservoirs intended for energy purposes, which leads to a distortion, although not very significant, of seasonal variations in the water level.

Additionally, the method of aggregated signal made it possible to recognize a low-frequency harmonic with a period of 12.85 yr. The period value itself is estimated from the sample 15 yr long, of course, with a high error. Nevertheless, the presence of a high-amplitude low-frequency variation in the aggregated signal compels one to at least try to interpret it. The closeness of this period to the known period of solar activity suggests the idea of a climatic origin of such a variation and its relation to cyclic components of global climatic variations. Comparison of the plots of the aggregated signal and daily Wolf numbers presented in Fig. 2 does not permit inferences to be made about a simple linear relation between low-frequency variations in the sea level and changes in solar activity. However, it should be taken into account that the solar activity variation is a broadband signal, and its influence on processes in the atmosphere is nonlinear. Therefore, it would be unreasonable to expect the periods and phases of low-frequency variations in the Caspian Sea level to coincide exactly with the Wolf numbers. A reliable conclusion about the relation of low-frequency variations in sea level to global variations in the climate can be based only on a thorough processing of long-term meteorological and hydrologic observations in the Caspian Sea basin.

REFERENCES

1. V. Kh. German, “Spectral Analysis of Variations in the Levels of the Azov, Black, and Caspian Seas in the Frequency Range from One Cycle in a Few Hours to One Cycle in a Few Days,” Tr. Gos. Okeanogr. Inst., No. 103, 52–73 (1970).
2. A. A. Lyubushin, “Classification of the States of Low-Frequency Geophysical Monitoring Systems,” Fiz. Zemli, No. 7, 135–141 (1994).
3. A. A. Lyubushin, “Analysis of Canonical Coherence Levels in Geophysical-Monitoring Problems,” Fiz. Zemli, No. 1, 59–66 (1998).

4. G. Nicolis and I. Prigogine, *Exploring Complexity, An Introduction* (Freedman, New York, 1989).
5. A. A. Lyubushin, "Aggregate Signal of Low-Frequency Geophysical Monitoring Systems," Fiz. Zemli, No. 3, 69–74 (1998).
6. A. A. Lyubushin, "Wavelet-Aggregated Signal and Synchronous Spikes in Problems of Geophysical Monitoring and Prediction of Earthquakes," Fiz. Zemli, No. 3, 20–30 (2000).
7. A. A. Lyubushin, V. F. Pisarenko, M. V. Bolgov, and T. A. Rukavishnikova, "Study of General Effects of River Runoff Variations," Meteorol. Gidrol., No. 7, 76–88 (2003).
8. G. Jenkins and D. G. Watts, *Spectrum Analysis and Its Applications* (Holden Day, San Francisco, 1968).
9. E. J. Hannan, *Multiple Time Series* (Wiley, New York, 1970).
10. D. R. Brillinger, *Time Series. Data Analysis and Theory* (Holt, Rinehart and Winston, New York, 1975).
11. S. L. Marple, Jr., *Digital Spectral Analysis with Applications* (Prentice-Hall, Englewood Cliffs, New Jersey, 1987).
12. *Marine Hydrometeorology and Hydrochemistry*, vol. VI, *Caspian Sea* (Gidrometeoizdat, St. Petersburg, 1992) [in Russian].
13. *Caspian Sea: Hydrology and Hydrochemistry* (Nauka, Moscow, 1986) [in Russian].
14. A. B. Rabinovich, "Calculation of Seiches of the Caspian Sea," Vestn. Mosk. Univ., Ser. Geogr., No. 4, 116–121 (1973).

Translated by N. Nazarenko